

Reaction of Samarium 1,4-Diaza-1,3-diene Complexes with Ketones: Generation of a New Versatile Tridentate Ligand via 1,3-Dipolar Cycloaddition

Joachim Scholz,^{*,†} Helmar Görls,[‡] Herbert Schumann,[§] and Roman Weimann[§]

Institut für Chemie, Universität Koblenz-Landau, Rheinau 1, D-56075 Koblenz, Germany, Institut für Anorganische und Analytische Chemie, Friedrich-Schiller-Universität Jena, Lessingstrasse 8, D-07743 Jena, Germany, and Institut für Anorganische und Analytische Chemie, Technische Universität Berlin, Strasse des 17. Juni 135, D-10623 Berlin, Germany

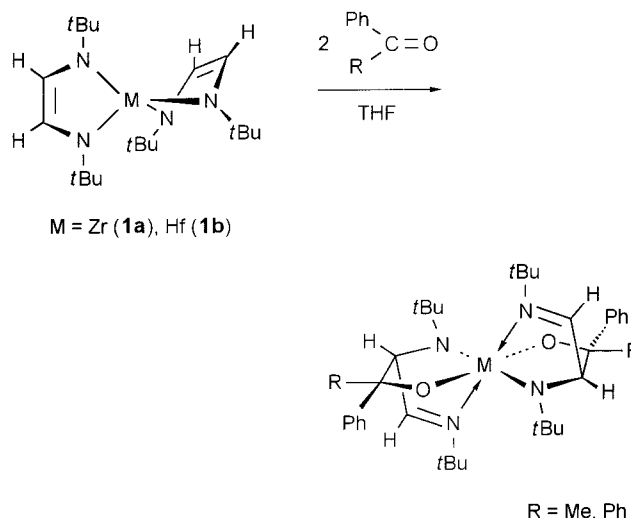
Received April 19, 2001

Treatment of $\text{SmI}_2(\text{THF})_n$ with the dilithium 1,4-diaza-1,3-diene (DAD) compound $\text{Li}_2\text{[(tBu)NCH=CHN(tBu)]}$ ($\equiv \text{Li}_2(\text{tBu-DAD})$; **2**) prepared by reduction of *t*Bu-DAD by 2 equiv of lithium in THF surprisingly results in the formation of the samarium(III) iodide complex $[(\text{THF})_2\text{Li}(\text{tBu-DAD})][(\text{THF})\text{Li}(\text{tBu-DAD})]\text{SmI}$ (**5**). The characteristic structural feature of **5** is formed by two (*Z*)-1,4-diaza-but-2-ene-1,4-diyl units bridging the Sm^{3+} with two Li^+ ions. Complex **5** and the analogous chloride complex $[(\text{THF})\text{Li}(\text{tBu-DAD})]_2\text{Sm}(\mu\text{-Cl})_2\text{Li}(\text{THF})_2$ (**4b**) react with 2 equiv of benzophenone to give the structurally very similar samarium complexes $\{[\text{OC}(\text{Ph})_2\text{CH}\{\text{CH}=\text{N}(\text{tBu})\}\text{N}(\text{tBu})]\text{Li}\}_2\text{SmX}(\text{THF})$ ($\text{X} = \text{Cl}$ (**6**), I (**7**)) in high yield. The reaction formally proceeds via a 1,3-dipolar cycloaddition of the benzophenone $\text{C}=\text{O}$ bond across a $\text{Sm}-\text{N}-\text{C}=\text{}$ fragment of the enediamide samarium complexes **4b** and **5**, including the formation of a new $\text{C}-\text{C}$ bond, and results in the formation of the novel tripodal ligand $[\text{OC}(\text{Ph})_2\text{CH}\{\text{CH}=\text{N}(\text{tBu})\}\text{N}(\text{tBu})]^{2-}$. X-ray structure determinations of **6** and **7** revealed that the two tripodal ligands and the halogen atom form a slightly distorted octahedral coordination geometry around the Sm^{3+} ion and that the Li^+ ions are retained within the ligand sphere by close contacts to their N and O atoms. By controlled hydrolysis of the cycloaddition product **6**, the new tripodal ligands can be separated from the samarium and isolated in the form of the lithium compound $\{[\text{OC}(\text{Ph})_2\text{CH}\{\text{CH}=\text{N}(\text{tBu})\}\text{N}(\text{tBu})]\text{Li}\}_2$ (**8**). The crystal structure of **8**, which is dimeric in the solid state, is reported.

Introduction

One of the most interesting and useful aspects of transition-metal centers in organometallic chemistry is that they can induce unusual transformations in coordinated ligands. $\text{C}-\text{C}$ bond-forming reactions have attracted special attention in this respect and have found application in metal-directed organic synthesis.¹ Recently, we reported on the novel reaction of early-transition-metal DAD² complexes with ketones.³ We had found that DAD ligands bonded to early transition metals can be selectively functionalized by forming a new $\text{C}-\text{C}$ bond between one of the imine carbon atoms and a carbon atom of the electrophilic substrate. Thus, the reaction of ketones with $(\text{tBu-DAD})_2\text{M}$ ($\text{M} = \text{Zr}$ (**1a**), Hf (**1b**)) leads to complexes in which the metal atom is octahedrally coordinated by two novel tridentate ligands (Scheme 1).

Scheme 1. Reaction of $(\text{tBu-DAD})_2\text{M}$ ($\text{M} = \text{Zr}$, Hf) with Ketones



[†] Universität Koblenz-Landau.

[‡] Friedrich-Schiller-Universität Jena.

[§] Technische Universität Berlin.

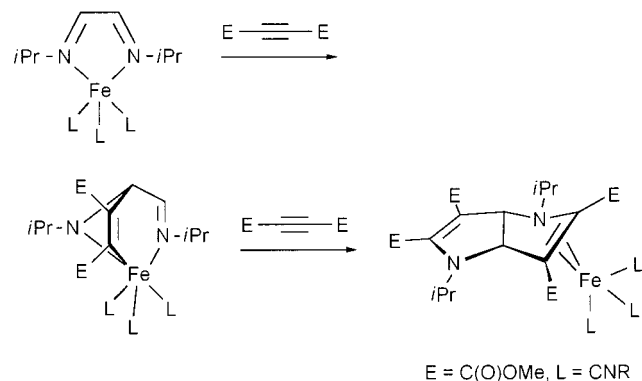
(1) (a) Braterman, P. S., Ed. *Reactions of Coordinated Ligands*; Plenum Press: New York, 1986; Vol. 1. (b) Collman, J. P.; Hegedus, L. S.; Norton, J. R.; Finke, G. R. *Principles and Applications of Organotransition Metal Chemistry*; University Science Books: Mill Valley, CA, 1987.

(2) Throughout this paper the 1,4-diaza-1,3-dienes in general are abbreviated as DAD. 1,4-Diaza-1,3-dienes of the formula $\text{RN}=\text{CHCH}=\text{NR}$ are abbreviated as R-DAD; hence, $(\text{tBu})\text{N}=\text{CHCH}=\text{N}(\text{tBu})$ is abbreviated as *t*Bu-DAD.

(3) Scholz, J.; Görls, H. *Inorg. Chem.* **1996**, 35, 4378–4382.

With respect to the metallacyclic nature of the reaction product and in view of the results of Frühauf et al., this reaction may be described as a 1,3-dipolar cycloaddition.⁴ In a series of papers Frühauf et al. reported that complexes such as $(\text{iPr-DAD})\text{FeL}_3$ ($\text{L} =$

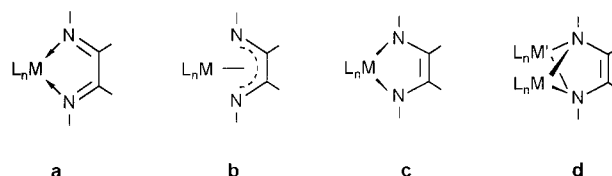
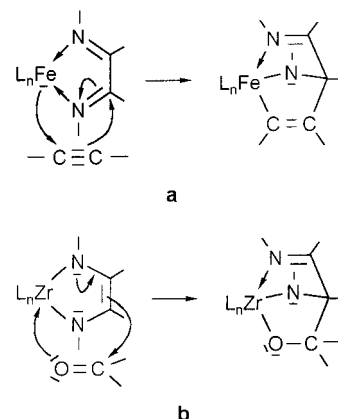
(4) Frühauf, H.-W. *Chem. Rev.* **1997**, 97, 523–596.

Scheme 2. Reaction Steps in the Cycloaddition of Alkynes to the Fe–N=C Fragment in the Complexes (DAD)Fe(L)₃

CO, RNC), containing a σ^2 -N,N'-chelating DAD ligand, react with organic substrates, e.g. alkynes, to give different C–C coupling products (Scheme 2).⁵ In the initial step the dipolarophilic alkyne adds across the Fe–N=C fragment of the DAD complex, resulting in the formation of a [2.2.1] bicyclic intermediate. On the basis of the isolobal analogy⁶ between the Fe–N=C fragment and the azomethine ylide, a classical organic 1,3-dipole, the initial step was described as an oxidative 1,3-dipolar [3 + 2] cycloaddition reaction. Moreover, Frühauf et al. have demonstrated that the Fe–N=C fragment is comparable with an electron-rich nucleophilic dipole that reacts preferentially with electron-deficient dipolarophiles such as the alkyne dimethyl acetylenedicarboxylate (Scheme 2).⁵ In the next step this [2.2.1] intermediate can further react with a second dipolarophile, forming a double cycloaddition product.

(5) 1,3-Dipolar cycloaddition reactions of Fe-, Ru-, and Mn(DAD) complexes were reported in the following publications. (a) Part 1: Frühauf, H.-W.; Seils, F.; Romao, M. J.; Goddard, R. J. *Angew. Chem.* **1983**, *95*, 1014–1015. (b) Part 2: Frühauf, H.-W.; Seils, F.; Goddard, R. J.; Romao, M. J. *Organometallics* **1985**, *4*, 948–949. (c) Part 3: Frühauf, H.-W.; Seils, F. J. *Organomet. Chem.* **1986**, *302*, 59–64. (d) Part 4: Frühauf, H.-W.; Seils, F. J. *Organomet. Chem.* **1987**, *323*, 67–76. (e) Part 5: Frühauf, H.-W.; Seils, F.; Stam, C. H. *Organometallics* **1989**, *8*, 2338–2343. (f) Part 6: De Lange, P. P. M.; Frühauf, H.-W.; van Wijnkoop, M.; Vrieze, K.; Wang, Y.; Heijdenrijk, D.; Stam, C. H. *Organometallics* **1990**, *9*, 1691–1694. (g) Part 7: Van Wijnkoop, M.; de Lange, P. P. M.; Frühauf, H.-W.; Vrieze, K.; Wang, Y.; Goubitz, K.; Stam, C. H. *Organometallics* **1992**, *11*, 3607–3617. (h) Part 8: De Lange, P. P. M.; Frühauf, H.-W.; Kraakman, M. J. A.; van Wijnkoop, M.; Kranenburg, M.; Groot, A. H. J. P.; Vrieze, K.; Fraanje, J.; Wang, Y.; Numan, M. *Organometallics* **1993**, *12*, 417–427. (i) Part 9: Van Wijnkoop, M.; Siebenlist, R.; de Lange, P. P. M.; Frühauf, H.-W.; Smeets, W. J. J.; Spek, A. L. *Organometallics* **1993**, *12*, 4172–4181. (j) Part 10: De Lange, P. P. M.; van Wijnkoop, M.; Frühauf, H.-W.; Vrieze, K.; Goubitz, K. *Organometallics* **1993**, *12*, 428–439. (k) Part 11: De Lange, P. P. M.; de Boer, R. P.; van Wijnkoop, M.; Frühauf, H.-W.; Vrieze, K.; Smeets, W. J. J.; Spek, A. L.; Goubitz, K. *Organometallics* **1993**, *12*, 440–453. (l) Part 12: De Lange, P. P. M.; Alberts, E.; van Wijnkoop, M.; Frühauf, H.-W.; Vrieze, K. J. *Organomet. Chem.* **1994**, *465*, 241–249. (m) Part 13: Van Wijnkoop, M.; Siebenlist, R.; Ernsting, J. M.; de Lange, P. P. M.; Frühauf, H.-W.; Horn, E.; Spek, A. L. J. *Organomet. Chem.* **1994**, *482*, 99–109. (n) Part 14: Feiken, N.; Frühauf, H.-W.; Vrieze, K.; Fraanje, J.; Goubitz, K. *Organometallics* **1994**, *13*, 2825–2832. (o) Part 15: Van Wijnkoop, M.; De Lange, P. P. M.; Frühauf, H.-W.; Vrieze, K.; Smeets, W. J. J.; Spek, A. L. *Organometallics* **1995**, *14*, 4781–4791. (p) Part 16: Feiken, N.; Frühauf, H.-W.; Vrieze, K.; Veldman, N.; Spek, A. L. J. *Organomet. Chem.* **1996**, *511*, 281–291. (q) Part 17: Feiken, N.; Schreuder, P.; Siebenlist, R.; Frühauf, H.-W.; Vrieze, K.; Kooijman, H.; Veldman, N.; Spek, A. L.; Fraanje, J.; Goubitz, K. *Organometallics* **1996**, *15*, 2148–2169. (r) Part 18: Siebenlist, R.; de Beurs, M.; Feiken, N.; Frühauf, H.-W.; Vrieze, K.; Kooijman, H.; Veldman, N.; Lakin, M. T.; Spek, A. L. *Organometallics* **2000**, *19*, 3032–3053.

(6) (a) Hoffmann, R. *Angew. Chem.* **1982**, *94*, 725–737; *Angew. Chem., Int. Ed. Engl.* **1982**, *21*, 711–723.

Chart 1. Structures of Complexes with N,N'-Chelating DAD Ligands: (a) σ^2 (4e Donor); (b) σ^2 (Radical Anion); (c) σ^2, π (Enediamide); (d) μ - σ^2, π (Bridging Enediamide)**Scheme 3.** Schematic Representation of the 1,3-Dipolar Cycloaddition (a) of (DAD)Fe(L)₃ to Alkynes and (b) of (DAD)ZrL₂ to Ketones

However, although the products of the reaction of **1a** and **1b** with ketones and that of the reaction of (iPr-DAD)Fe(CNR)₃ with alkynes show similar structural features, there are some facts which suggest that the mechanism of their formation must be different: In contrast to the low-valent iron complexes (iPr-DAD)-FeL₃ (L = CO, RNC), where a neutral DAD ligand is bonded to the central metal, forming a planar five-membered metallacycle (Chart 1, **a**),⁷ for DAD complexes of the early transition metals the “folded envelope geometry” is well-established. Thus, the DAD bonding situation in **1a** and **1b** is best described by a σ^2, π -enediamide structure with extensive dianionic character of the heterodiene, as shown by **c** in Chart 1.⁸

Furthermore, since the high valent d⁰ metal centers of the formally unsaturated eight-electron complexes **1a** and **1b** exhibit an appreciable Lewis acidity, the M–N=C= fragment prefers to react with dipolarophiles containing a strongly nucleophilic part such as ketones. Finally, the cycloaddition reaction of (iPr-DAD)FeL₃ results in the oxidation of Fe⁰ to Fe²⁺, whereas for **1a** and **1b** the oxidation state of the transition metal (+4) does not change (Scheme 3).

Thus, to provide additional insight regarding the mechanism of the cycloaddition reaction and the factors that might be used to influence this process, a study of the reaction of the DAD complexes of lanthanides with ketones was undertaken.

In contrast to the DAD complexes of early and late transition metals, relatively little is known about DAD

(7) (a) van Koten, G.; Vrieze, K. *Adv. Organomet. Chem.* **1982**, *21*, 151–239. (b) Vrieze, K. J. *Organomet. Chem.* **1986**, *300*, 307–326.

(8) (a) Chamberlain, L. R.; Durfee, L. D.; Fanwick, P. E.; Kobriger, L. M.; Latesky, St. L.; McMullen, A. K.; Steffey, B. D.; Rothwell, I. P.; Folting, K.; Huffman, J. C. *J. Am. Chem. Soc.* **1987**, *109*, 6068–6076. (b) Galindo, A.; Ienco, A.; Mealli, C. *New J. Chem.* **2000**, *14*, 73–75.

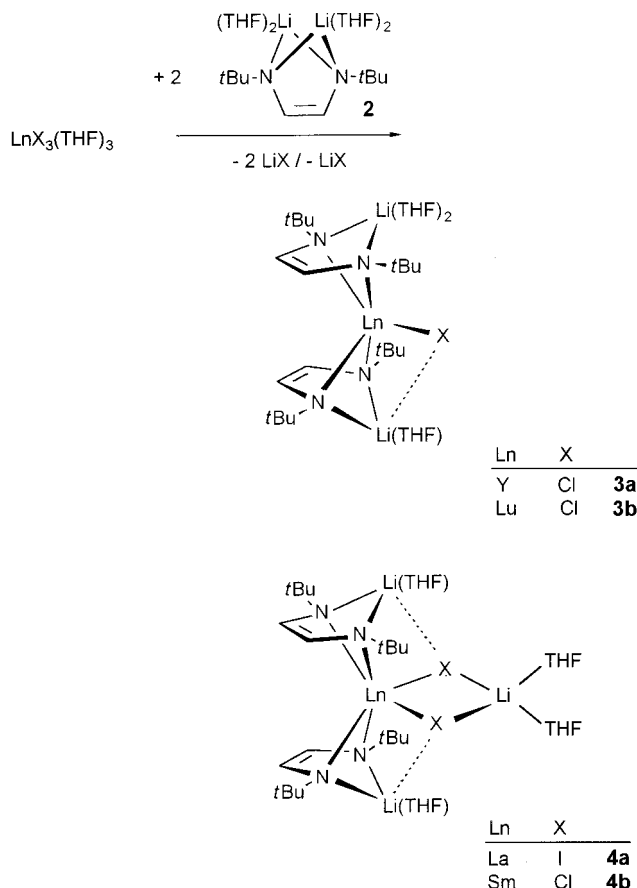
complexes of the lanthanides. It has been shown that a variety of lanthanide metal vapors react with *t*Bu-DAD to yield the homoleptic complexes $\text{Ln}(\text{tBu-DAD})_3$ ($\text{Ln} = \text{Y}, \text{Nd}, \text{Sm}, \text{Eu}, \text{Gd}, \text{Ho}, \text{Yb}$).⁹ The room-temperature X-ray crystallographic results and the magnetic susceptibility of $\text{Yb}(\text{tBu-DAD})_3$ at higher temperature are consistent with the formulation of an Yb^{3+} center and three N,N'-coordinated radical anions $(\text{tBu-DAD})^-$ (Chart 1, **b**).^{9c} Similar bonding situations have been observed for the DAD complexes $\text{Cp}^*_2\text{M}(\text{DAD})$ ($\text{M} = \text{Sm}$,^{10a} Y^{10b}) and $(\text{COT})\text{Sm}(\text{DAD})(\text{THF})$.^{10c} More recently we have found that $[(\text{tBu-DAD})\text{Li}]^-$ units may act as cyclopentadienyl-like ligands in organolanthanide complexes.¹¹ For example, reaction of the THF adducts of the lanthanide halogenides LnX_3 ($\text{Ln} = \text{La}, \text{Sm}, \text{Lu}, \text{Y}$) with the dilithium DAD compound $\text{Li}_2(\text{tBu-DAD})$ (**2**)¹² in a molecular ratio of 1:2 yields the complexes $[(\text{THF})_2\text{Li}(\text{tBu-DAD})][(\text{THF})\text{Li}(\text{tBu-DAD})]\text{LnCl}$ ($\text{Ln} = \text{Y}$ (**3a**), Lu (**3b**)) and $[(\text{THF})\text{Li}(\text{tBu-DAD})]_2\text{Ln}(\mu\text{-X})_2\text{Li}(\text{THF})_2$ ($\text{Ln} = \text{La}$, $\text{X} = \text{I}$ (**4a**); $\text{Ln} = \text{Sm}$, $\text{X} = \text{Cl}$ (**4b**), Scheme 4), whose structure is featured by the two heterodienes which are coordinated in their enediamide form bridging the lanthanide with two lithium ions (Chart 1, **d**).

Certainly, owing to their structural relationship with the cyclopentadienyl lanthanide halides Cp^*_2LnCl and $\text{Cp}^*_2\text{Ln}(\mu\text{-Cl})_2\text{Li}(\text{THF})_2$ ($\text{Cp}^* \equiv \text{C}_5\text{Me}_5$),¹³ respectively, these new lanthanide DAD complexes **3a,b** and **4a,b** are of interest as starting materials in organolanthanide chemistry. In this paper we present our initial results on the reaction of these lanthanide DAD complexes with benzophenone. Altogether, the studies reported here focus on gaining a better insight into the overall mechanism of 1,3-dipolar reactivity.

Results and Discussion

Synthesis of $[(\text{THF})_2\text{Li}(\text{tBu-DAD})][(\text{THF})\text{Li}(\text{tBu-DAD})]\text{SmI}$ (5**).** As the structural features of the lanthanide(III) complexes with $[(\text{tBu-DAD})\text{Li}]^-$ ligands are very similar to those of the cyclopentadienyl complexes, it should also be possible to prepare the analogue of the divalent samarium complex $\text{Cp}^*_2\text{Sm}(\text{THF})_x$ ($x = 0$,^{14a} 1,^{14b} 2^{14c}). The original cause for this investigation was to produce the samarium(II) complex $[(\text{THF})_2\text{Li}(\text{tBu-DAD})]_2\text{Sm}$, which was expected to provide access to a

Scheme 4. Syntheses of the Lanthanide DAD Complexes
 $[(\text{THF})_2\text{Li}(\text{tBu-DAD})][(\text{THF})\text{Li}(\text{tBu-DAD})]\text{LnCl}$ ($\text{Ln} = \text{Y}$ (**3a**), Lu (**3b**)) and
 $[(\text{THF})\text{Li}(\text{tBu-DAD})]_2\text{Ln}(\mu\text{-X})_2\text{Li}(\text{THF})_2$ ($\text{Ln} = \text{La}$, $\text{X} = \text{I}$ (**4a**); $\text{Ln} = \text{Sm}$, $\text{X} = \text{Cl}$ (**4b**))



wide range of unusual reactions, as has been done by the metallocene complex Cp^*_2Sm .¹⁵

Slow addition of 2 equiv of $\text{Li}_2(\text{tBu-DAD})$ (**2**) (generated in situ from *t*Bu-DAD and lithium at room temperature in THF)^{11a,12} to a suspension of SmI_2 in THF gives a red-violet product which is obtained in 64% yield. However, the reaction of SmI_2 with $\text{Li}_2(\text{tBu-DAD})$ is unusual: the red-violet color of the isolated product suggested that the samarium(II) metal center was oxidized to the trivalent state and a qualitative halogen test indicated the presence of iodine. Moreover, the results of the combustion analysis data and an X-ray crystal structure (vide infra) revealed that instead of the expected samarium(II) complex the new complex $[(\text{THF})_2\text{Li}(\text{tBu-DAD})][(\text{THF})\text{Li}(\text{tBu-DAD})]\text{SmI}$ (**5**) had been formed (Scheme 5).

(9) (a) Cloke, F. G. N.; de Lemos, H. C.; Sameh, A. A. *J. Chem. Soc., Chem. Commun.* **1986**, 1344–1345. (b) Cloke, F. G. N. *Chem. Soc. Rev.* **1993**, 17–24. (c) Bochkarev, M. N.; Trifonov, A. A.; Cloke, F. G. N.; Dalby, C. I.; Matsunaga, P. T.; Andersen, R. A.; Schumann, H.; Loebel, J.; Hemling, H. *J. Organomet. Chem.* **1995**, *486*, 177–182.

(10) (a) Recknagel, A.; Noltemeyer, M.; Edelmann, F. T. *J. Organomet. Chem.* **1991**, *410*, 53–61. (b) Scholz, A.; Thiele, K.-H.; Scholz, J.; Weimann, R. *J. Organomet. Chem.* **1995**, *501*, 195–200. (c) Poremba, P.; Edelmann, F. T.; *J. Organomet. Chem.* **1997**, *549*, 101–104.

(11) (a) Görls, H.; Neumüller, B.; Scholz, A.; Scholz, J. *Angew. Chem.* **1995**, *107*, 732–735; *Angew. Chem., Int. Ed. Engl.* **1995**, *34*, 673–676. (b) Trifonov, A. A.; Zakharov, L. N.; Bochkarev, M. N.; Struchkov, Y. T. *Izv. Akad. Nauk, Ser. Khim.* **1994**, 148–151.

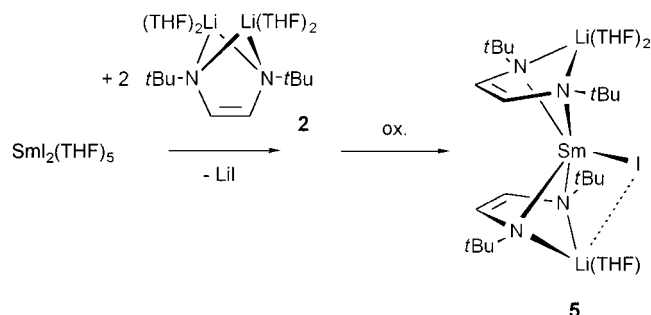
(12) Haaf, M.; Schmiedl, A.; Schmedake, T. A.; Powell, D. R.; Millevolte, A. J.; Denk, M.; West, R. *J. Am. Chem. Soc.* **1998**, *120*, 12714–12719.

(13) (a) Schumann, H.; Meese-Marktscheffel, J. A.; Esser, L. *Chem. Rev.* **1995**, *95*, 865–886. (b) Evans, W. J.; Foster, S. E. *J. Organomet. Chem.* **1992**, *433*, 79–94.

(14) (a) Evans, W. J.; Hughes, L. A.; Hanusa, T. P. *Organometallics* **1986**, *5*, 1285–1291. (b) Evans, W. J.; Kociok-Köhn, G.; Foster, S. E.; Ziller, J. W.; Doedens, R. J. *J. Organomet. Chem.* **1993**, *444*, 61–66. (c) Evans, W. J.; Grate, J. W.; Choi, H. W.; Bloom, I.; Hunter, W. E.; Atwood, J. L. *J. Am. Chem. Soc.* **1985**, *107*, 941–946.

(15) Selected examples illustrating the reactivity of Cp^*_2Sm : (a) Evans, W. J. *Polyhedron* **1987**, *6*, 803–835. (b) Evans, W. J.; Ulibarri, T. A.; Ziller, J. W. *J. Am. Chem. Soc.* **1988**, *110*, 6877–6879. (c) Evans, W. J.; Drummond, D. K.; Chamberlain, L. R.; Doedens, R. J.; Bott, S. G.; Zhang, H.; Atwood, J. L. *J. Am. Chem. Soc.* **1988**, *110*, 4983–4994. (d) Evans, W. J.; Drummond, D. K. *J. Am. Chem. Soc.* **1989**, *111*, 3329–3335. (e) Evans, W. J.; Ulibarri, T. A.; Ziller, J. W. *J. Am. Chem. Soc.* **1990**, *112*, 2314–2324. (f) Evans, W. J.; Kociok-Köhn, G.; Leong, V. S.; Ziller, J. W. *Inorg. Chem.* **1992**, *31*, 3592–3600. (g) Evans, W. J.; Gonzales, S. L.; Ziller, J. W. *J. Am. Chem. Soc.* **1994**, *116*, 2600–2608. (h) Evans, W. J.; Rabe, G. W.; Ziller, J. W.; Doedens, R. J. *Inorg. Chem.* **1994**, *33*, 2719–2726. (i) Evans, W. J.; Seibel, C. A.; Ziller, J. W. *Inorg. Chem.* **1998**, *37*, 770–776.

Scheme 5. Synthesis of [(THF)₂Li(*t*Bu-DAD)][(THF)Li(*t*Bu-DAD)]SmI (5)



Complex **5** has a simple ¹H NMR spectrum consisting of broad single lines for the *tert*-butyl (δ 0.30) and imine protons (δ 8.58) and signals caused by the coordinated THF (δ 3.63, 1.77). Equivalence of the *t*Bu-DAD ligands in the ¹³C NMR spectrum, as exemplified by single resonances at δ 59.65 and 28.09 (CMe₃) and at δ 127.30 (HC=CH), also indicates that **5** has *C*_{2v} molecular symmetry in solution. As expected, although the signals of the ¹H and the ¹³C NMR spectra are observed at chemical shifts similar to those of **4b**,^{11a} the paramagnetic nature of this complex hindered full interpretation of the spectra. Definitive formulation of the bonding situation of the heterodiene ligands was provided by a single-crystal X-ray structure analysis.

Consistent with the other known lanthanide complexes with [Li(*t*Bu-DAD)][−] ligands,¹¹ the structural analysis of **5** (Figure 1, Table 2) revealed a monomeric complex with a coordination sphere of the Sm(III) center composed of four nitrogen atoms of two chelating enediame dianions and the iodide. The four nitrogen atoms bridge the samarium with two lithium ions. The bonding parameters within the two heterodiene ligands are not different from those of the analogous samarium chloride complex **4b**^{11a} and show a pronounced "long–short–long" sequence of the N–C=C–N bond length (N11–C16 = 1.399(12) Å, C15–C16 = 1.350(14) Å, N12–C15 = 1.401(13) Å, N21–C25 = 1.401(12) Å, C25–C26 = 1.371(14) Å, N22–C26 = 1.406(12) Å), which is typical for an enediame structure. Moreover, the short distances between the olefinic carbon atoms C15 and C16 and the metal centers Li1 and Sm as well as the close contacts of Li2 to C25 and C26 (2.23(2) and 2.24(2) Å) lie in the range of usual Li–C¹⁶ and Sm–C¹⁷ bonds and indicate an intensive π interaction: thus, one heterodiene dianion is formally η^4 coordinated to Sm and Li1 and the other η^4 coordinated to Li2, respectively. However, the structure of **5** significantly differs from that of **4b** in that complex **5** has not added an extra LiI molecule and therefore the central samarium atom does not achieve the coordination number 6. Nevertheless, an intramolecular contact between Li2 and the iodide (2.887(16) Å) which is only slightly longer than the Li–I distance of [LiI(pmedien)] (2.75(3) and 2.67(3) Å)^{18a} or [LiI(NC₅H₃-3,5-Me₂)₃] (2.80(1) Å)^{18b} strongly affects the Sm–I distance: this bond length of 3.362(1) Å is not only significantly longer than the terminal Sm–I dis-

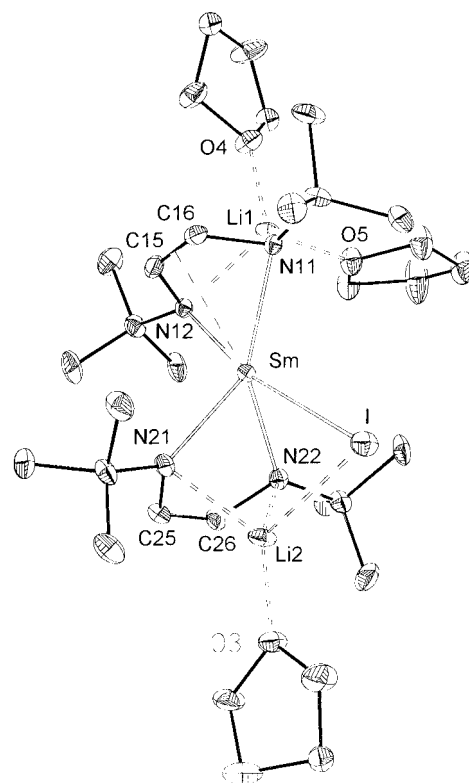


Figure 1. ORTEP representation of the molecular structure of **5**. Thermal ellipsoids are shown at the 40% probability level, and hydrogen atoms are omitted for clarity.

Table 1. Selected Structural Parameters for [(THF)₂Li(*t*Bu-DAD)][(THF)Li(*t*Bu-DAD)]SmI (5)

Bond Distances (Å)					
Sm–N11	2.399(8)	Sm–N12	2.361(7)	Sm–N21	2.315(8)
Sm–N22	2.339(8)	Sm–C15	2.654(10)	Sm–C16	2.688(10)
Sm–I	3.362(1)	Li2–I	2.887(16)	Li1–N11	2.102(18)
Li1–N12	2.141(18)	Li1–C15	2.485(19)	Li1–C16	2.478(20)
Li2–N21	2.163(20)	Li2–N22	2.195(19)	Li2–C25	2.230(20)
Li2–C26	2.244(20)	Li1–O4	1.960(18)	Li1–O5	2.000(19)
Li2–O3	1.909(18)	N11–C16	1.399(12)	N12–C15	1.401(13)
C15–C16	1.350(14)	N21–C25	1.401(12)	N22–C26	1.406(12)
C25–C26	1.371(14)				
Bond Angles (deg)					
N21–Sm–N22	72.73(28)	N11–Sm–N12	72.78(25)		
Li1–Sm–Li2	159.81(48)				
Interplanar Angles (deg)					
(N11, Sm, N12)(N21, Sm, N22)				87.3(3)	

tances of Cp*₂SmI(THF) (3.043(2) Å)^{19a} and Cp*₂SmI–(C₆H₁₀N₄) (3.100(2) Å)^{19b} as is typical for bridging vs terminal ligands but also longer than those of the iodide-bridged diiminophosphinate samarium(III) complex [Ph₂P(NSiMe₃)₂]₂Sm(μ -I)₂Li(THF)₂ (3.161(1) and 3.162(1) Å).²⁰ The fact that the reaction of SmI₂(THF)₅ with Li₂(*t*Bu-DAD) is accompanied by an oxidation of the sa-

(16) A distance of 2.50 Å has been discussed as an upper limit for a Li–C interaction: Zarges, W.; Marsch, M.; Harms, K.; Koch, W.; Frenking, G.; Boche, G. *Chem. Ber.* **1991**, *124*, 543–549.

(17) The Sm–(C=C) distances in **5** are comparable with the average Sm–C_{sp} distances of 2.68(1)–2.80(1) Å of Cp*₂Sm^{III} complexes.¹³

(18) (a) [LiI(pmedien)] (pmedien = [Me₂N(CH₂CH₂)₂NMe], 2.75(3), 2.67(3) Å: Raston, C. L.; Skelton, B. W.; Whitaker, C. R.; White, A. H. *J. Chem. Soc., Dalton Trans.* **1988**, 987–990. (b) [LiI(NC₅H₃-3,5-Me₂)₃], 2.80(1) Å: Raston, C. L.; Whitaker, C. R.; White, A. H. *J. Chem. Soc., Dalton Trans.* **1988**, 991–995.

(19) (a) Evans, W. J.; Grate, J. W.; Levan, K. R.; Bloom, I.; Peterson, T. T.; Doedens, R. J.; Zhang, H.; Atwood, J. L. *Inorg. Chem.* **1986**, *25*, 3614–3619. (b) Evans, W. J.; Drummond, D. K.; Hughes, L. A.; Zhang, H.; Atwood, J. L. *Polyhedron* **1988**, *7*, 1693–1703.

(20) Recknagel, A.; Steiner, A.; Noltemeyer, M.; Brooker, S.; Stalke, D.; Edelman, F. T. *J. Organomet. Chem.* **1991**, *414*, 327–335.

marium(II) center has not been fully understood to this day, but it has been observed in other reactions of divalent samarium also: for instance, reaction of $\text{SmI}_2 \cdot (\text{THF})_5$ with the lithium diiminophosphinate compound $\text{Li}(\text{THF})_2[\text{Ph}_2\text{P}(\text{NSiMe}_3)_2]^{20}$ or with the lithium salt of 2-(phenylamino)-4-(phenylimino)-2-pentene, $\text{Li}[\text{PhN}=\text{CMeCH}=\text{CMeNPh}]$,²¹ always leads to samarium(III) complexes, irrespective of the stoichiometric ratio of the reagents.

Reaction of $[(\text{THF})\text{Li}(t\text{Bu-DAD})]_2\text{Sm}(\mu\text{-Cl})_2\text{Li}(\text{THF})_2$ (4b**) and $[(\text{THF})_2\text{Li}(t\text{Bu-DAD})][(\text{THF})\text{Li}(t\text{Bu-DAD})]\text{SmI}$ (**5**) with Benzophenone.** The reaction of the samarium DAD complex **4b** with 2 equiv of benzophenone was carried out in diethyl ether at room temperature. As the reaction proceeds, the solution initially acquires a dark green color which changes to pale yellow. Furthermore, the concomitant formation of a precipitate (LiCl) was observed. The reaction produced a single new product (**6**) isolated as colorless prisms from diethyl ether. Preliminary qualitative analysis tests indicated the presence of both chlorine and lithium in this product, and the combustion analysis was consistent with the formula $\{[\text{OC}(\text{Ph})_2\text{CH}\{\text{CH}=\text{N}(t\text{Bu})\}-\text{N}(t\text{Bu})]\text{Li}\}_2\text{SmCl}(\text{THF})$ (**6**) (Scheme 6).

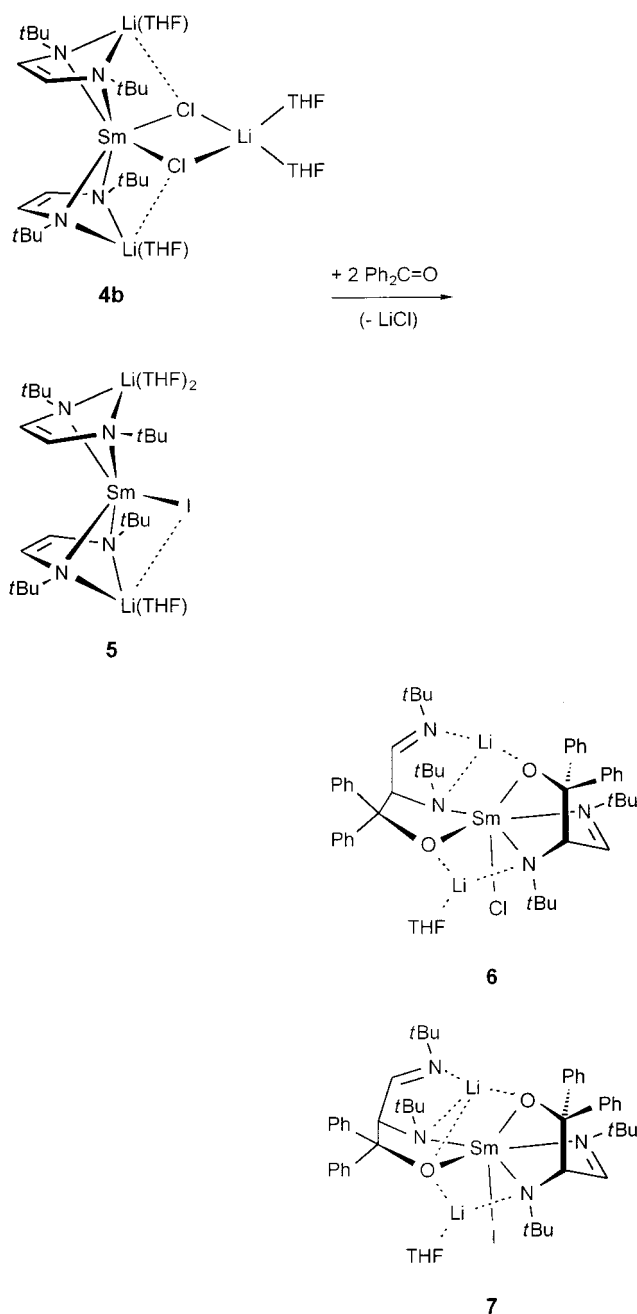
Complex **6** is air- and moisture-sensitive and soluble in aromatic solvents and ethers. Unfortunately, at room temperature it shows a very complicated ^1H NMR spectrum, which is uninformative due to numerous resonances combined with partial line broadening and strong paramagnetic shifts. However, these NMR data suggest that **6** exhibits a high asymmetry even in solution.

The reaction of the samarium iodide complex **5** with benzophenone carried out under identical conditions as reported above at first resulted also in a transient color change of the reaction mixture from red-violet to dark green. Unfortunately, as in the case of the reaction of **4b**, we were not successful in characterizing the dark green intermediate, which is perhaps a simple coordination adduct of the samarium DAD complex. Finally, complex **7** was isolated as an analytically pure colorless solid by crystallization from diethyl ether in 68% yield.

The large number of resonances in the ^1H NMR spectrum of **7** is consistent with a complete lack of symmetry of **7** on the NMR time scale. Moreover, the spectrum shows the same signal pattern and chemical shifts nearly identical with those observed for **6**. Close examination of the number of signals in the ^1H NMR spectra of **6** and **7** suggests that a second isomer must be present in nearly equal amount in the solution of **6** as well as of **7**. In view of the solid-state structures of **6** and **7** (vide infra), we speculate that the second isomer may be another diastereomer.

To understand the molecular geometries and the structural parameters of the new tripodal ligand, the X-ray crystal structures of **6** and **7** were determined. Single crystals of both compounds were obtained from diethyl ether solutions at -20°C . Selected bond lengths and angles are given in Table 2, experimental crystallographic data are summarized in Table 4, and perspective views are presented in Figures 2 and 3. Further data are available in the Supporting Information.

Scheme 6. Reaction of $[(\text{THF})\text{Li}(t\text{Bu-DAD})]_2\text{Sm}(\mu\text{-Cl})_2\text{Li}(\text{THF})_2$ (4b**) and $[(\text{THF})_2\text{Li}(t\text{Bu-DAD})][(\text{THF})\text{Li}(t\text{Bu-DAD})]\text{SmI}$ (**5**) with Benzophenone**



The samarium atom is surrounded by two dianionic tripodal ligands $[\text{OC}(\text{Ph})_2\text{CH}\{\text{CH}=\text{N}(t\text{Bu})\}\text{N}(t\text{Bu})]^{2-}$ arising from the cycloaddition reaction of benzophenone to the $\text{Sm}-\text{N}-\text{C}=\text{C}$ moiety of the enediamide ligands of **4b** and **5**. However, only one of these ligands is coordinated by the three donor functions O1, N1, and N2, resulting in a [2.2.1] bicyclic structure motive. The bridgehead positions are occupied by the samarium atom and the C-C-coupled former imine carbon atom C2. As a consequence of the cycloaddition reaction N2 and C2 have changed their hybridization into sp^3 (sum of angles at N2: **6** at $338.8(2)^\circ$; **7** at $337.2(5)^\circ$; sum of angles at C2: **6** at $329.9(3)^\circ$; **7** at $330.8(5)^\circ$) and now display regular tetrahedral geometry. Furthermore, the atoms of the starting enediamide skeleton $\text{N1}-\text{C1}=\text{C2}-\text{N2}$ are

(21) Drees, D.; Magull, J. *Z. Anorg. Allg. Chem.* **1994**, 620, 814–818.

Table 2. Selected Structural Parameters for $\{[\text{OC}(\text{Ph})_2\text{CH}\{\text{CH}=\text{N}(\text{tBu})\}\text{N}(\text{tBu})]\text{Li}\}_2\text{SmCl}(\text{THF})$ (**6**) and $\{[\text{OC}(\text{Ph})_2\text{CH}\{\text{CH}=\text{N}(\text{tBu})\}\text{N}(\text{tBu})]\text{Li}\}_2\text{SmI}(\text{THF})$ (**7**)

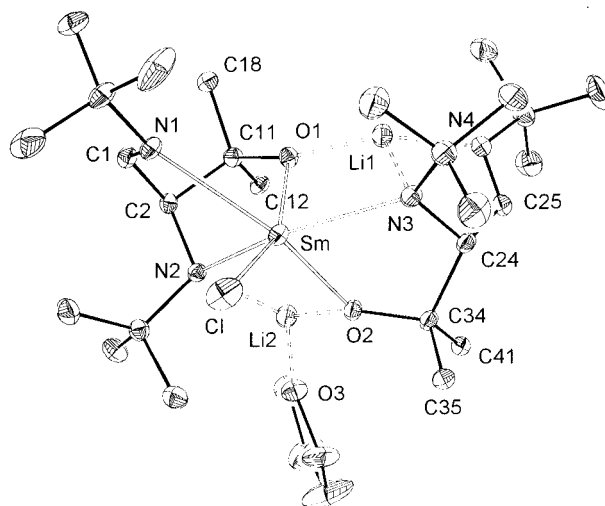
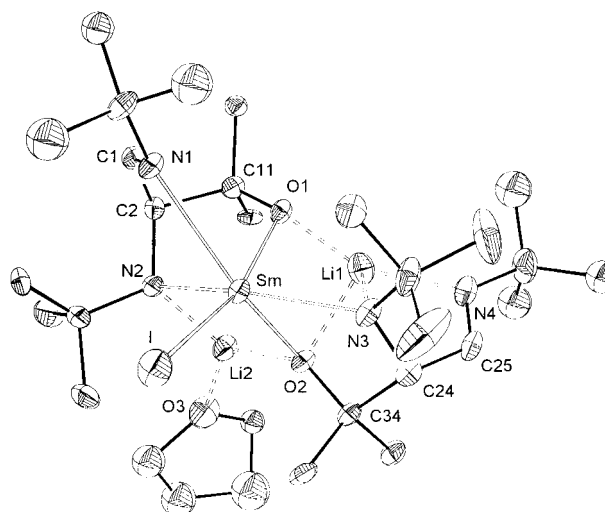
	6	7		6	7		6	7
Bond Distances (Å)								
Sm–N1	2.679(3)	2.709(6)	Sm–N2	2.406(3)	2.438(5)	Sm–N3	2.406(3)	2.350(6)
Sm–O1	2.323(2)	2.304(5)	Sm–O2	2.282(2)	2.457(4)	Sm–Cl(I)	2.692(1)	3.137(1)
N1–C1	1.266(4)	1.272(9)	N2–C2	1.470(4)	1.490(9)	C1–C2	1.519(4)	1.503(10)
C2–C11	1.572(4)	1.585(9)	O1–C11	1.400(4)	1.397(8)	N3–C24	1.459(4)	1.467(8)
C24–C25	1.527(5)	1.537(10)	N4–C25	1.264(4)	1.267(10)	C24–C34	1.609(4)	1.587(10)
O2–C34	1.396(4)	1.413(8)	Li1–N3	2.036(7)	2.271(14)	Li1–N4	1.992(7)	2.009(15)
Li2–N2	2.071(7)	2.108(13)	Li1–O1	1.784(6)	1.844(15)	Li1–O2		2.047(14)
Li2–O2	1.891(6)	1.943(12)	Li2–O3	1.972(7)	1.978(13)			
Bond Angles (deg)								
N1–Sm–N2	70.58(8)	71.05(18)	N1–Sm–O1	74.19(8)	74.80(17)	N2–Sm–O1	70.13(8)	71.20(17)
N2–Sm–N3	136.66(9)	142.14(18)	N1–Sm–O2	147.12(8)	142.06(16)	N1–Sm–O2	147.12(8)	142.06(16)
N2–Sm–O2	78.63(8)	79.71(17)	N3–Sm–O1	78.83(8)	85.12(18)			

Table 3. Selected Structural Parameters for $\{[\text{OC}(\text{Ph})_2\text{CH}\{\text{CH}=\text{N}(\text{tBu})\}\text{N}(\text{tBu})]\text{Li}\}_2$ (**8**)

		Bond Distances (Å)			
Li–N1	2.120(4)	Li–N2	2.109(5)	Li–O	1.988(4)
Li–OA	1.792(4)	N1–C1	1.268(3)	N2–C2	1.466(3)
C1–C2	1.487(3)	C2–C3	1.593(3)	O–C3	1.368(3)
		Bond Angles (deg)			
N1–Li–N2	83.6(2)	N1–Li–O		98.4(2)	
N2–Li–O	79.8(2)	Li–O–LiA		79.2(2)	
O–Li–OA	100.8(2)	Li–N1–C1		100.0(2)	
Li–N2–C2	90.5(2)	Li–O–C3		110.5(2)	
LiA–O–C3	158.4(2)	O–C3–C2		107.7(2)	
N1–C1–C2	122.2(2)	C1–C2–N2		111.8(2)	
C1–C2–C3	108.2(2)	C3–C2–N2		106.4(2)	

no longer in the same plane and the observed N–C distances are longer in the amide fragments (N2–C2: **6**, 1.470(4) Å; **7**, 1.490(9) Å) than in the imine groups (N1–C1: **6**, 1.266(4) Å; **7**, 1.272(9) Å). The second tripodal ligand chelates the samarium center only by the amidato nitrogen atom N3 (Sm–N3: **6**, 2.406(3) Å; **7**, 2.350(6) Å) and the oxygen atom O2 (Sm–O2: **6**, 2.282(2) Å; **7**, 2.457(4) Å) to form a puckered five-membered ring with a "bite" angle N3–Sm–O2 of 68.99(9)° (**6**) and 65.08(16)° (**7**), respectively, whereas the imine function N4 is coordinated to one of the lithium ions Li1 (Li1–N4: **6**, 1.992(7) Å; **7**, 2.009(15) Å).

An interesting structural feature of the cycloaddition products **6** and **7** is the bridging linkage of the lithium ions Li1 and Li2 with the ligand framework. Small differences between the molecular structures of **6** and **7** in this respect primarily may be ascribed to the steric effects of the halogen atoms. In both complexes the amidato nitrogen atom N2 of the tridentate ligand and the oxygen atom O2 of the bidentate ligand are bridged by the Li2(THF) moiety. In complex **7** the oxygen atom O2 is also bonded to the lithium ion Li1 (Li1–O2 = 2.047(14) Å), which in turn is attached in both complexes to the nitrogen atoms N3 and N4 of the bidentate ligand (Li1–N3: **6** at 2.036(7) Å, **7** at 2.271(14) Å; Li1–N4: **6** at 1.992(7) Å, **7** at 2.009(15) Å) and the oxygen atom O1 of the tridentate ligand (Li1–O1: **6** at 1.784(6) Å, **7** at 1.844(15) Å). Altogether, this close network of bridging interactions between the two tripodal ligands generates a hemispherical shield around the samarium center which perhaps is a prerequisite for the stability of the complexes. The Sm–halogenide distances (**6**, Sm–Cl = 2.692(1) Å; **7**, Sm–I = 3.137(1) Å) are not unusual and compare well with those observed in nonmetallocene samarium(III) complexes with terminally bonded

**Figure 2.** ORTEP representation of the molecular structure of **6**. Thermal ellipsoids are shown at the 40% probability level. For clarity, no hydrogen atoms and only the ipso carbon atoms of the phenyl groups are shown.**Figure 3.** ORTEP representation of the molecular structure of **7**. Thermal ellipsoids are shown at the 40% probability level. For clarity, no hydrogen atoms and only the ipso carbon atoms of the phenyl groups are shown.

chloride ($\{\text{O}(\text{SiPh}_2\text{O})_2\text{Li}(\text{dme})\}_2\text{SmCl}(\text{dme})$, 2.717(1) Å;^{22a} $\text{SmCl}_3(\text{THF})_4$, 2.635(3)–2.679(3) Å^{22b}) or iodide ligands ($(\text{ArO})_2\text{SmI}(\text{THF})_2$, 3.024(2) Å (Ar \equiv 2,6-(*t*Bu)₂-4-Me-C₆H₂);^{23a} $\{(\text{Me}_3\text{Si})\text{NC}(\text{tBu})\text{CH}(\text{SiMe}_3)\}_2\text{SmI}(\text{THF})$, 3.092(1) Å^{23b}).

Table 4. Summary of X-ray Diffraction Data and Overall Refinement Parameters for [(THF)₂Li(*t*Bu-DAD)][(THF)Li(*t*Bu-DAD)]SmI (5), {[OC(Ph)₂CH{CH=N(*t*Bu)}N(*t*Bu)]Li₂SmCl(THF) (6), {[OC(Ph)₂CH{CH=N(*t*Bu)}N(*t*Bu)]Li₂SmI(THF) (7), and {[OC(Ph)₂CH{CH=N(*t*Bu)}N(*t*Bu)]Li₂ (8)

	5	6	7	8
chem formula	C ₃₂ H ₆₄ N ₄ O ₃ ILi ₂ Sm	C ₅₀ H ₆₈ N ₄ O ₃ CLi ₂ Sm	C ₅₀ H ₆₈ N ₄ O ₃ ILi ₂ Sm	C ₄₆ H ₆₂ N ₄ O ₂ Li ₂
mol wt	844.02	972.79	1064.24	716.89
cryst dimens (mm ³)	0.15 × 0.40 × 0.20	0.40 × 0.38 × 0.36	0.22 × 0.18 × 0.12	0.32 × 0.30 × 0.28
cryst color, shape	red-violet prism	colorless prism	colorless prism	colorless prism
cryst syst	monoclinic	orthorhombic	orthorhombic	orthorhombic
space group	<i>P</i> 2 ₁ / <i>c</i> (No. 14)	<i>Pbca</i> (No. 61)	<i>P</i> 2 ₁ 2 ₁ 2 ₁ (No. 19)	<i>Pbca</i> (No. 61)
temp (°C)	−88	−90	−90	−90
cell params				
<i>a</i> (Å)	11.472(4)	18.618(3)	11.0244(3)	17.268(2)
<i>b</i> (Å)	14.608(3)	20.007(2)	20.0222(6)	12.748(2)
<i>c</i> (Å)	23.844(6)	26.098(5)	22.9007(9)	19.842(2)
β (deg)	99.64(3)			
<i>V</i> (Å ³)	3939.3(18)	9721(2)	5054.9(3)	4367(1)
no. of formula units <i>Z</i>	4	8	4	4
calcd density <i>D_c</i> (g cm ^{−3})	1.423	1.329	1.398	1.090
abs coeff μ(Mo Kα) (cm ^{−1})	22.41	13.06	18.14	0.66
scan type	φ-scan	φ-scan	φ-scan	
min/max transmissn	0.743/0.995	0.218/0.278	0.691/0.811	
<i>F</i> (000)	1708	4040	2164	1552
<i>hkl</i> range	0−12, 0−15, −25 to +25	0−24, 0−25, −33 to 0	−14 to +11, −23 to +26, −24 to +29	0−24, −17 to 0, 0−27
2θ range (deg)	1.28–44.84	4.82–54.84	6.36–55.02	4.48–59.98
no. of unique total data	5665	11 065	23 095	6353
no. of indep data	4646	11 065	11 289	6352
<i>R</i> _{int}	0.045	0.067	0.034	
no. of obsd data with <i>F</i> _o > 4σ(<i>F</i> _o)	3868	6717	8128	2391
no. of params	385	550	556	368
restraints	0	0	18	0
<i>R</i> ₁ _{obsd}	0.055	0.033	0.057	0.062
<i>wR</i> ₂ _{obsd}	0.137	0.076	0.104	0.140
<i>R</i> ₁ _{all} ^a	0.0958	0.0958	0.095	0.0958
<i>wR</i> ₂ _{all} ^b	0.1178	0.1178	0.117	0.1178
goodness of fit	1.112	1.072	1.010	1.144
largest diff peak and hole (e Å ^{−3})	1.569/−0.895	0.594/−0.637	0.610/−0.938	0.243/−0.223

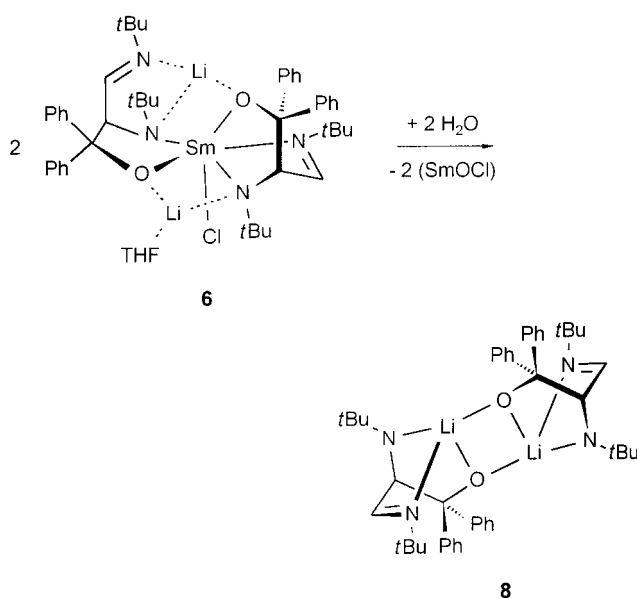
^a *R*₁ = (Σ||*F*_o| − |*F*_c||)/Σ|*F*_o|. ^b *wR*₂ = [Σ(*wF*_o² − *F*_c²)²]/Σ(*wF*_o²)^{1/2}.

Hydrolysis of {[OC(Ph)₂CH{CH=N(*t*Bu)}N(*t*Bu)]Li₂SmCl(THF) (6). As mentioned above, solutions of **6** and **7** are sensitive to air and moisture. To further explore the reactivity of these species and to learn more about the robustness of the newly generated tripodal ligand in view of its further application in organometallic and coordination chemistry, controlled hydrolysis of **6** was performed: after addition of 2 equiv of H₂O to a stirred solution of **6** in diethyl ether the reaction mixture became cloudy and a white solid precipitated. Colorless crystals of the new compound **8** were isolated in reasonable yield after careful filtration of the reaction mixture and concentration of the filtrate with subsequent cooling to −30 °C.

The room temperature ¹H and ¹³C NMR spectra of the air- and moisture-sensitive compound **8** recorded in THF-*d*₈ are in agreement with the structure consisting of a 2-(*tert*-butylamino)-3-(*tert*-butylimino)-1,1-diphenylpropanolate anion, which is coordinated by the three donor atoms to the lithium ion (Scheme 7).

In the ¹H NMR spectrum the methine protons of the ligand backbone give rise to two doublets at very different positions: One doublet appears at δ 7.30,

Scheme 7. Hydrolysis of {[OC(Ph)₂CH{CH=N(*t*Bu)}N(*t*Bu)]Li₂SmCl(THF) (6)



(22) (a) Lorenz, V.; Fischer, A.; Jacob, K.; Brüser, W.; Edelmann, F. T. *Chem. Eur. J.* **2001**, 7, 848–857. (b) Anfang, S.; Karl, M.; Faza, N.; Massa, W.; Magull, J.; Dehnicke, K. *Z. Anorg. Allg. Chem.* **1997**, 623, 1425–1432.

(23) (a) Hou, Z.; Fujita, A.; Yoshimura, T.; Jesorka, A.; Zhang, Y.; Yamazaki, H.; Wakatsuki, Y. *Inorg. Chem.* **1996**, 35, 7190–7195. (b) Hitchcock, P. B.; Lappert, M. F.; Tian, S. *J. Organomet. Chem.* **1997**, 549, 1–12.

which is in the typical range of imine protons. The other proton resonates at δ 4.75, which reflects a change in hybridization from sp² to sp³, resulting from the cycloaddition reaction. The ³J_{H–H} coupling between these methine protons is rather small (2.0 Hz), indicating a larger dihedral angle between the C–H bonds as a

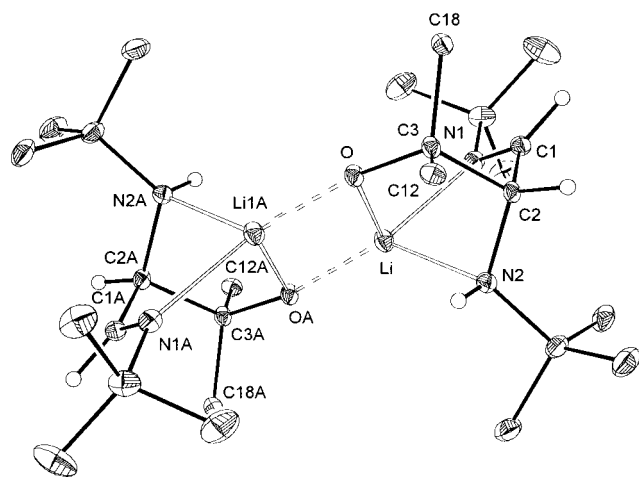


Figure 4. ORTEP representation of the molecular structure of **8**. Thermal ellipsoids are shown at the 40% probability level. For clarity, only the hydrogen atoms bound to C1, C2, and N2 and only the ipso carbon atoms of the phenyl groups are shown.

consequence of the distorted [2.2.1] bicyclic geometry. Interestingly, the N–H proton signal appears as a rather sharp singlet at δ 1.42.

In the ^{13}C NMR spectrum the signal of the C–C-coupled bridgehead methine carbon atom is observed at δ 62.83, which is a normal value for an sp^3 -hybridized carbon nucleus substituted by an amine function. The signals of the adjacent carbon atoms of the ligand backbone appear at δ 165.40, consistent with an intact imine function, and at δ 82.92, indicating the striking change of the former benzophenone carbonyl carbon atom.

Complex **8** crystallizes as prismatic crystals in the orthorhombic space group *Pbca* with four dimers in the unit cell. The complex is best described as an intramolecularly coordinated imine–amine adduct of a lithium alcoholate dimer containing a central four-membered Li_2O_2 ring core (Figure 4). The O-lithiated 2-(*tert*-butylamino)-3-(*tert*-butylimino)-1,1-diphenylpropanolate anion acts as a tridentate ligand, chelating the lithium ion and bridging the other lithium ion through the oxygen atom, achieving 4-fold coordination of the alkaline metal. Selected geometrical parameters are given in Table 3. The Li–O distances vary considerably, the Li–O distance to the oxygen in the chelate ring of 1.988(4) Å being longer than the distance to the other oxygen atom of the Li_2O_2 ring core (1.792(4) Å).²⁴ Nevertheless, the Li_2O_2 unit is exactly planar, as required by the crystallographic symmetry. The Li–N1(imine) distance of 2.120(4) Å is comparable to the dative Li–N2(amine) bond distance of 2.109(5) Å and corresponds to that of other examples having a four-coordinate lithium atom.²⁵ The C2–C3 bond (1.593(3) Å) joining the benzophenone molecule with the amide carbon atom of the former DAD unit N1=C1–C2(H)–N2(H) is comparable with a regular C–C bond.²⁶

(24) Li–O bond distances of dimeric lithium complexes containing a Li_2O_2 ring core are as follows. (a) $[\text{MeCH}=\text{C}(\text{OtBu})\text{OLi}(\text{Me}_2\text{NCH}_2\text{CH}_2\text{NMe}_2)]_2$, Li–O = 1.945 and 1.906 Å: Seebach, D.; Amstutz, R.; Laube, T.; Schweizer, W. B.; Dunitz, J. D. *J. Am. Chem. Soc.* **1985**, *107*, 5403–5409. (b) $[\text{CH}_2=\text{C}(\text{tBu})\text{OLi}(\text{Me}_2\text{NCH}_2\text{CH}_2\text{N}(\text{H})\text{Me})]_2$, Li–O = 1.872 and 1.898 Å: Laube, T.; Dunitz, J. D.; Seebach, D. *Helv. Chim. Acta* **1985**, *68*, 1373–1393.

Furthermore, the bond distance of the reduced imine function N2–C2 (1.466(3) Å) is as expected for a C–N single bond,²⁶ while the N1–C1 bond of the intact imine function is somewhat shorter and is consistent with the presence of some degree of C–N double-bond character (1.268(3) Å).²⁶ Altogether, in the case of $\{[\text{OC}(\text{Ph})_2\text{CH}=\text{CH}=\text{N}(\text{tBu})\text{N}(\text{tBu})]\text{Li}\}_2$ (**8**) we succeeded in the isolation and structural characterization of a stable imine–amine-functionalized lithium alcoholate dimer which can be further used in the syntheses of other complexes with this new multidentate ligand system.

The reaction reported in this paper demonstrates for the first time that the coordination of dianionic 1,4-diaza-1,3-dienes to an electrophilic lanthanide ion results in the specific activation of the diimine skeleton itself and affords an opportunity for a subsequent C–C coupling reaction with ketones. In other words, the results presented here constitute the transformation of a dianionically bonded 1,4-diaza-1,3-diene to a tridentate N,O,N-bound ligand by addition of benzophenone, a strategy reported recently for zirconium and hafnium DAD complexes.³

Furthermore, it has been shown that the C–C coupling product can be easily displaced from the lanthanide complex as a lithium adduct of a 2-amine-3-imine-functionalized alcohol. Certainly, the synthesis of organic products such as 2-amine- or 3-imine-functionalized alcohols has been previously achieved by a variety of known methods.²⁷ However, the reaction of the samarium DAD complexes demonstrates their capability in organic synthesis and completes the series of C–H, C–C, and C–N coupling reactions which have been observed in DAD complexes.^{5,28} Further studies on the chemistry of DAD complexes of samarium and other lanthanides are in progress.

Experimental Section

General Considerations. All experiments were performed under an atmosphere of dry argon using standard Schlenk techniques. Solvents were distilled from sodium/benzophenone ketyl (THF, diethyl ether) or LiAlH_4 (pentane) under argon and stored over activated 4 Å molecular sieves. All glassware was thoroughly oven-dried or flame-dried under vacuum prior to use. Benzophenone was purchased from Aldrich Chemicals

(25) (a) $[\text{Li}(\text{tBu-DAD})_3\text{Nb}]$, Li–N(imine) = 2.07(2), 1.98(2) Å: Richter, B.; Scholz, J.; Sieler, J.; Thiele, K.-H. *Angew. Chem.* **1995**, *107*, 2865–2867; *Angew. Chem., Int. Ed. Engl.* **1995**, *34*, 2865–2867. (b) $[(\text{tBu-DAD})_2\text{Li}]$, Li–N(imine) = 2.134(7), 2.148(6) Å: Gardiner, M. G.; Hanson, G. R.; Henderson, M. J.; Lee, F. C.; Raston, C. L. *Inorg. Chem.* **1994**, *33*, 2456–2461. (c) $[\text{Li}\{\text{N}(\text{tBu})\text{CHCH}_2\text{N}(\text{tBu})\}_2\text{AlH}_2]$, Li–N(imine) = 2.11(1), 2.12(1) Å: Gardiner, M. G.; Lawrence, S. M.; Raston, C. L. *Inorg. Chem.* **1999**, *38*, 4467–4472.

(26) C–C = 1.530 Å, C–N = 1.469 Å, C=N = 1.279 Å: Allen, F. H.; Kennard, O.; Watson, D. G.; Brammer, L.; Orpen, A. G.; Taylor, R. *J. Chem. Soc., Perkin Trans. 2* **1987**, S1–S19. (b) tBu-DAD , C=N = 1.267(2) Å, C–C = 1.467(2) Å: Huige, C. J. M.; Spek, A. L.; de Boer, J. L. *Acta Crystallogr.* **1985**, *C41*, 113–116.

(27) (a) Synthesis of 2-amine- and 3-imine-functionalized alcohols using C–C bond forming reactions via organosamarium(III) intermediates: Murakami, M.; Ito, Y. *J. Organomet. Chem.* **1994**, *473*, 93–99. (b) A highly versatile and selective method for the intermolecular coupling of imines with aldehydes or ketones uses niobium(III) and tantalum(III) reagents, providing a diastereoselective route to α -amino alcohols: Roskamp, E. J.; Pedersen, S. F. *J. Am. Chem. Soc.* **1987**, *109*, 6551–6553. Takai, K.; Ishiyama, T.; Yasue, H.; Nobunaka, T.; Itoh, M.; Oshiki, T.; Mashima, K.; Tani, K. *Organometallics* **1998**, *17*, 5128–5132.

(28) tom Dieck, H.; Munz, C.; Ehlers, J. In *Organometallics in Organic Synthesis 2*; Springer-Verlag: Berlin, Heidelberg, New York, 1989; pp 21–43.

and used as received. $\text{SmI}_2(\text{THF})_5$,²⁹ $\text{SmCl}_3(\text{THF})_4$,³⁰ and *t*Bu-DAD³¹ were prepared according to literature procedures. NMR spectra were recorded in THF-*d*₈ on a Varian 300 BB (¹H NMR at 300.075 MHz, ¹³C NMR at 75.462 MHz) or a Varian UNITY 500 spectrometer (¹H NMR at 499.843 MHz, ¹³C NMR at 125.639 MHz) at 20 or 25 °C, unless indicated otherwise. ¹H and ¹³C NMR spectra were referenced internally using the residual solvent resonances (THF-*d*₈: δ_{H} 1.73, δ_{C} 25.2). ¹*J*_{C-H} values were obtained from gated ¹³C{¹H} NMR spectra. Elemental analyses were carried out by the analysis laboratory at the Martin-Luther-University of Halle-Wittenberg. Melting points are uncorrected.

[Li(THF)₂Li(*t*Bu-DAD)][(THF)Li(*t*Bu-DAD)]SmI (2). To a solution of *t*Bu-DAD (3.37 g, 20 mmol) in THF (50 mL) was added lithium metal (0.28 g, 40 mmol) at room temperature. The colorless solution rapidly took on the deep red color of the product and was stirred until the metal pieces had dissolved completely and the starting 1,4-diaza-1,3-diene *t*Bu-DAD had been converted quantitatively to **2** (ca. 10 h). The resulting solution was filtered and then used without further purification in the synthesis of **5**.

[(THF)₂Li(*t*Bu-DAD)][(THF)Li(*t*Bu-DAD)]SmI (5). To a suspension of $\text{SmI}_2(\text{THF})_5$ (7.65 g, 10 mmol) in THF (100 mL) was added dropwise a THF solution (50 mL) of **2** (20 mmol) at -30 °C. The solution was warmed to room temperature and stirred for 12 h, during which time the solution gradually became red-violet. The solvent was removed in vacuo and the resulting solid extracted with diethyl ether. The resulting red-violet solution was concentrated and cooled to -30 °C to yield red-violet crystalline **5** (5.32 g, 63%). ¹H NMR (THF-*d*₈, 300 MHz, 25 °C): δ 8.58 (br s, 4H, HC=CH), 3.63 (m, 12H, OCH₂-CH₂, THF), 1.77 (m, 12H, OCH₂CH₂, THF), 0.30 (br s, 36H, CMe₃). ¹³C{¹H} NMR (THF-*d*₈, 75 MHz, 25 °C): δ 127.30 (d, ¹*J*_{C-H} = 159 Hz, HC=CH), 68.15 (t, ¹*J*_{C-H} = 146 Hz, OCH₂-CH₂, THF), 59.65 (s, CMe₃), 28.09 (q, ¹*J*_{C-H} = 124 Hz, CMe₃), 26.27 (t, ¹*J*_{C-H} = 131 Hz, OCH₂CH₂, THF). Mp: 165 °C dec. Anal. Calcd for C₃₂H₆₄N₄O₃Li₂Sm: C, 45.54; H, 7.64; N, 6.64. Found: C, 45.30; H, 7.51; N, 6.75.

{[OC(Ph)₂CH{CH=N(*t*Bu)}N(*t*Bu)]Li₂SmCl(THF)} (6). A sample of [(THF)Li(*t*Bu-DAD)]₂Sm(μ -Cl)₂Li(THF)₂ (**4b**; 2.46 g, 3.0 mmol) was dissolved in diethyl ether (100 mL). Two equivalents of benzophenone (1.09 g, 6.0 mmol) was added at room temperature, and the mixture was stirred for 3 h. The precipitate (LiCl) was filtered off and the solution was concentrated under vacuum to about 50 mL. A colorless crystalline solid was obtained upon cooling the solution to -20 °C for several days. The product **6** (2.36 g, 81%) can be purified by recrystallization from diethyl ether. ¹H NMR (THF-*d*₈, 300 MHz, 25 °C): δ 9.00–4.20 (br, m, Ph), 3.58 (m, OCH₂CH₂, THF), 2.20 (s), 2.02 (s), 1.89 (s), 1.74 (m, OCH₂CH₂, THF), 1.17 (br s, CMe₃), 0.03 (s), -0.23 (s), -1.81 (s), -2.73 (s), -7.80 (br, s). Mp: 120 °C dec. Anal. Calcd for C₅₀H₆₈N₄O₃ClLi₂Sm: C, 61.73; H, 7.45; N, 5.76. Found: C, 61.60; H, 7.40; N, 5.83.

{[OC(Ph)₂CH{CH=N(*t*Bu)}N(*t*Bu)]Li₂SmI(THF)} (7). Following the procedure described for **6**, 2.53 g (3.0 mmol) of [(THF)₂Li(*t*Bu-DAD)][(THF)Li(*t*Bu-DAD)]SmI (**5**) was reacted with 1.09 g (6.0 mmol) of benzophenone. The reaction mixture was filtered, concentrated, and cooled to -20 °C to provide 2.75 g (86%) of colorless crystalline **7**. ¹H NMR (THF-*d*₈, 300 MHz, 25 °C): δ 9.10–4.15 (br, m, Ph), 3.61 (m, OCH₂CH₂, THF),

2.23 (s), 2.07 (s), 1.94 (s), 1.77 (m, OCH₂CH₂, THF), 1.20 (br s, CMe₃), 0.33 (s), 0.06 (s), -0.19 (s), -1.78 (s), -2.72 (s), -7.49 (br, s). Mp: 136 °C dec. Anal. Calcd for C₅₀H₆₈N₄O₃Li₂Sm: C, 56.43; H, 6.44; N, 5.26. Found: C, 56.12; H, 6.50; N, 5.35.

{[OC(Ph)₂CH{CH=N(*t*Bu)}N(*t*Bu)]Li₂} (8). To a solution of **6** (2.00 g, 2.0 mmol) in THF (50 mL) were added via syringe 72 μ L of degassed water (4.0 mmol) at 20 °C. The solution was stirred for 2 h. The solvent was removed in vacuo and the resulting white solid extracted with diethyl ether. The extract was concentrated and cooled to -30 °C to yield colorless crystalline **8** (1.08 g, 75%). ¹H NMR (THF-*d*₈, 300 MHz, 25 °C): δ 7.87 (d, 2H, *o*-C₆H₅), 7.79 (d, 2H, *o*-C₆H₅), 7.30 (d, ³*J*_{H-H} = 2.0 Hz, 1H, N=CHCH), 7.20–6.85 (m, 12H, *m*/*p*-C₆H₅), 4.75 (d, ³*J*_{H-H} = 2.0 Hz, 1H, N=CHCH), 1.42 (s, 1H, NH), 1.12 (s, 9H, CMe₃), 0.83 (s, 9H, CMe₃). ¹³C NMR (THF-*d*₈, 75 MHz, 25 °C): δ 165.40 (dd, ¹*J*_{C-H} = 160.4 Hz, ²*J*_{C-H} = 6.8 Hz, N=CHCH), 154.69, 153.38 (s, *ipso*-C₆H₅), 128.31, 127.93, 127.68, 127.63 (d, *o*/*m*-C₆H₅), 126.22 (d, *p*-C₆H₅), 82.92 (s, LiOC), 62.83 (dd, ¹*J*_{C-H} = 136.2 Hz, ²*J*_{C-H} = 12.9 Hz, N=CHCH), 57.59, 51.47 (s, CMe₃), 30.57 (q, ¹*J*_{C-H} = 124.4 Hz, CMe₃), 29.52 (q, ¹*J*_{C-H} = 125.1 Hz, CMe₃). Mp: 98–99 °C. Anal. Calcd for C₂₃H₃₁N₂OLi: C, 77.07; H, 8.72; N, 7.82. Found: C, 76.91; H, 8.84; N, 7.91.

X-ray Data Collection, Structure Determination, and Refinement. The intensity data for the compounds **5**, **6**, and **8** were collected on a Nonius CAD4 diffractometer and those for the compound **7** on a Nonius Kappa CCD diffractometer, using graphite-monochromated Mo K α radiation. Data were corrected for Lorentz, polarization, and absorption effects. No absorption correction was made for **8**.^{32,33} The structures were solved by direct methods (SHELXS)³⁴ and refined by full-matrix least-squares techniques against *F*_o² (SHELXL-97).³⁵ Only for the compound **8** were the hydrogen atoms located by difference Fourier synthesis and refined isotropically. The hydrogen atoms of the other structures were included at calculated positions with fixed thermal parameters. All non-hydrogen atoms were refined anisotropically.³⁵ XP (SIEMENS Analytical X-ray Instruments, Inc.) was used for structure representations.

Further details of the crystal structure investigations are available on request from the director of the Cambridge Crystallographic Data Center, 12 Union Road, GB–Cambridge CB2 1EZ, U.K., on quoting the depository numbers CCSD-150838 (**5**), CCSD-150836 (**6**), CCSD-150835 (**7**), and CCSD-150837 (**8**), the names of the authors, and the journal citation.

Acknowledgment. Financial support for this research was provided by the Deutsche Forschungsgemeinschaft and Bayer AG, Leverkusen, Germany. We are also grateful to Prof. Dr. D. Steinborn (Martin-Luther-Universität Halle-Wittenberg) for providing laboratory facilities. We thank Dr. F. Girgsdies (Technische Universität Berlin) for help with the X-ray diffraction analyses.

Supporting Information Available: Listings of atomic coordinates, thermal parameters, and bond distances and angles for complexes **5**–**8**. This material is available free of charge via the Internet at <http://pubs.acs.org>.

OM010323J

(29) (a) Girard, P.; Namy, J. L.; Kagan, H. B. *J. Am. Chem. Soc.* **1980**, *102*, 2693–2698. (b) Evans, W. J.; Gummersheimer, T. S.; Ziller, J. W. *J. Am. Chem. Soc.* **1995**, *117*, 8999–9002.

(30) Anhydrous SmCl_3 was prepared following a standard procedure and then transformed into the corresponding THF adduct: (a) Freeman, J. H.; Smith, M. L. *J. Inorg. Nucl. Chem.* **1958**, *7*, 224–227. (b) Manzer, L. E. *Inorg. Synth.* **1982**, *21*, 135–140.

(31) Kligman, J. M.; Barnes, R. K. *Tetrahedron*, **1970**, *26*, 2555–2560.

(32) MOLEN, An Interactive Structure Solution Procedure; Enraf-Nonius, Delft, The Netherlands, 1990.

(33) Otwinowski, Z.; Minor, W. Processing of X-ray Diffraction Data Collected in Oscillation Mode. In *Methods in Enzymology*; Carter, C. W., Sweet, R. M., Eds.; Academic Press: New York, 1997; Vol. 276 (Macromolecular Crystallography, Part A), pp 307–326.

(34) Sheldrick, G. M. *Acta Crystallogr.* **1990**, *A46*, 467–473.

(35) Sheldrick, G. M. SHELXL-97; University of Göttingen, Göttingen, Germany, 1993.